

Dalton Transactions

An international journal of inorganic chemistry

Accepted Manuscript

This article can be cited before page numbers have been issued, to do this please use: N. Wiratpruk, A. Noor, C. McLean, P. S. Donnelly and P. Barnard, *Dalton Trans.*, 2020, DOI: 10.1039/C9DT04687A.



This is an Accepted Manuscript, which has been through the Royal Society of Chemistry peer review process and has been accepted for publication.

Accepted Manuscripts are published online shortly after acceptance, before technical editing, formatting and proof reading. Using this free service, authors can make their results available to the community, in citable form, before we publish the edited article. We will replace this Accepted Manuscript with the edited and formatted Advance Article as soon as it is available.

You can find more information about Accepted Manuscripts in the [Information for Authors](#).

Please note that technical editing may introduce minor changes to the text and/or graphics, which may alter content. The journal's standard [Terms & Conditions](#) and the [Ethical guidelines](#) still apply. In no event shall the Royal Society of Chemistry be held responsible for any errors or omissions in this Accepted Manuscript or any consequences arising from the use of any information it contains.

Charge Neutral Rhenium Tricarbonyl Complexes of Tridentate N-Heterocyclic Carbene Ligands that Bind to Amyloid Plaques of Alzheimer's Disease

View Article Online
DOI: 10.1039/C9DT04687A

Nuchareenat Wiratpruk,^a Asif Noor,^b Catriona A. McLean,^c Paul S. Donnelly^y and Peter J. Barnard^{a*}

^a*Department of Chemistry and Physics, La Trobe Institute for Molecular Science, La Trobe University, Victoria, 3086, Australia.*

^b*School of Chemistry and Bio21 Molecular Science and Biotechnology Institute, University of Melbourne, Parkville, Victoria, 3010, Australia.*

^c*Florey Institute of Neuroscience and Mental Health, University of Melbourne, Parkville, Victoria, 3010, Australia*

Abstract

Two tridentate ligand systems bearing *N*-heterocyclic carbene (NHC), amine and carboxylate donor groups coupled to benzothiazole- or stilbene-based amyloid binding moieties were synthesised. Reaction of the imidazolium salt containing pro-ligands with $\text{Re}(\text{CO})_5\text{Cl}$ yielded the corresponding rhenium metal complexes which were characterised by NMR, and X-ray crystallography. These ligands are of interest for the potential preparation of technetium-99m imaging agents for Alzheimer's disease and the capacity of these rhenium complexes bind to amyloid fibrils composed of amyloid- β peptide and amyloid plaques in human frontal cortex brain tissue was evaluated using fluorescence microscopy. These studies show that the complexes bound efficiently to amyloid- β fibrils and some evidence of binding to amyloid- β plaques.

Introduction

Alzheimer's disease (AD) is a progressive neurodegenerative disease characterised by severe memory loss and disturbances in cognitive and behavioural functions.¹ The pathological mechanism of AD remains unknown, however the formation of insoluble plaques in the brain composed of the amyloid- β peptide are believed to play an important role in the progression of this disease.² Therefore, evaluation and quantification of the amyloid- β plaque load using targeted radiopharmaceutical diagnostic agents offer the potential for the early diagnosis of AD.³

Positron emission tomography (PET) and single photon emission computed tomography (SPECT) are the two most common nuclear imaging techniques that use radioactive tracers to diagnose diseases.⁴ These techniques allow for the non-invasive visualisation of disease progression at various levels ranging from molecular to whole organ.⁵ PET radiotracers require positron emitting radionuclides such as ^{11}C ($t_{1/2} = 20.3$ mins) and ^{18}F ($t_{1/2} = 109.8$ mins), whereas SPECT radiotracers

require gamma emitting radionuclides such as ^{99m}Tc ($t_{1/2} = 6.06$ hours) and ^{123}I ($t_{1/2} = 13.2$ hours).^{6, 7} Even though SPECT has a lower sensitivity and resolution compared to PET, it is widely available in many hospitals and for the commonly used isotope ^{99m}Tc there is no requirement for an onsite cyclotron.^{8, 9} Therefore, the development of SPECT radiotracers labelled with ^{99m}Tc for the diagnosis AD offers the potential for an easily accessible and affordable nuclear medicine technique for the early detection of this disease.¹⁰⁻¹²

Metal complexes of *N*-heterocyclic carbene (NHC) ligands have been extensively studied for a range of applications, including as homogeneous chemical catalysts,¹³ luminescent and electroluminescent materials¹⁴ and as potential medicinal agents.¹⁵ Despite their outstanding properties as ligands, less work has been directed towards the use of NHCs for the development of diagnostic imaging agents based on metallic radionuclides. We are interested in the preparation of new NHC ligands for radiopharmaceutical applications and previously we reported the first example of labelling an NHC ligand with the ^{99m}Tc (in the form of $^{99m}\text{Tc}(\text{CO})_3$).¹⁶ As part of this research, we have studied the chemistry of the $\text{Re}(\text{CO})_3$ core with bidentate and tridentate NHC ligands.^{16, 17} Che and co-workers reported early examples of $\text{Re}(\text{CO})_3$ complexes of NHC ligands e.g. **I**,¹⁸ while more recently, $\text{Re}(\text{CO})_3$ complexes with bidentate pyridyl-, quinoliny- and pyrimidyl-functionalized NHC ligands e.g. **II**, and **III** and **IV** have been described (Figure 1).^{19, 20}

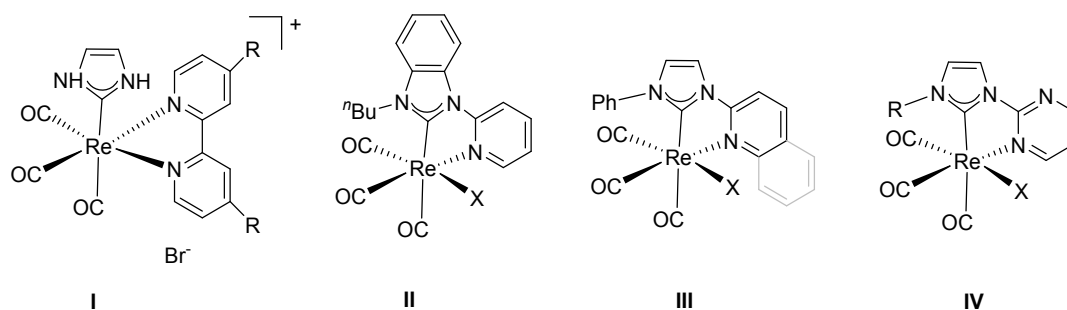
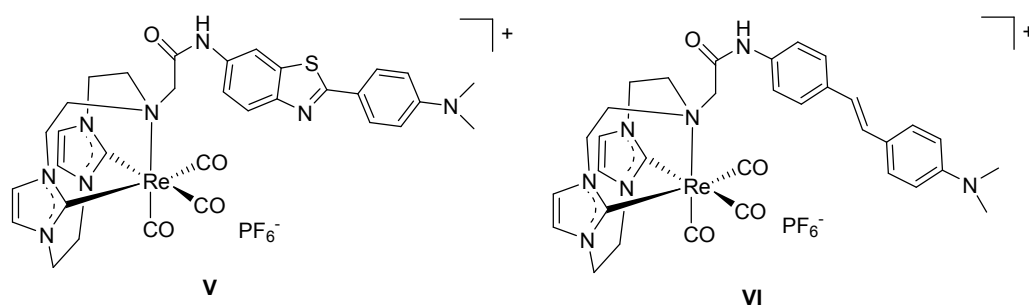


Figure 1. Examples of $\text{Re}(\text{CO})_3$ complexes with *N*-heterocyclic carbene ligands.

Previously we reported a series of $\text{Re}(\text{CO})_3$ complexes of bifunctional *bis*(NHC)-amine ligands coupled to benzothiazole- **V** and stilbene-based **VI** amyloid binding moieties (Figure 2).²¹ These complexes were highly stable in ligand challenge experiments with histidine and cysteine and bound to amyloid fibrils composed of the amyloid- β peptide. In addition, epi-fluorescence microscopy studies showed that **VI** bound selectively to amyloid plaques in human Alzheimer's disease brain tissue.²¹ Despite these promising results, complexes of this type are unlikely to be useful for radiopharmaceutical applications as the cationic charge associated with complex **VI** is likely to impede its passage through the blood brain barrier.²²



View Article Online
DOI: 10.1039/C9DT04687A

Figure 2. Structures of Re complexes of cyclic *bis*(NHC)-amine ligands coupled to benzothiazole- **V** and (b) stilbene-based **VI** amyloid binding moieties.

In an effort to improve the potential application of *N*-heterocyclic carbene ligand of the $\text{Re}(\text{CO})_3 / \text{Tc}(\text{CO})_3$ core for radiopharmaceutical applications, the synthesis of a new series of tridentate ligands that combine a NHC unit with amine and carboxylate donors to produce neutral complexes with the $\text{M}(\text{CO})_3$ core are reported herein. These ligands have been coupled to benzothiazole- and stilbene-based amyloid binding moieties and the capacity of the $\text{Re}(\text{CO})_3$ complexes to bind to amyloid fibrils and amyloid plaques in human frontal cortex brain tissue are evaluated.

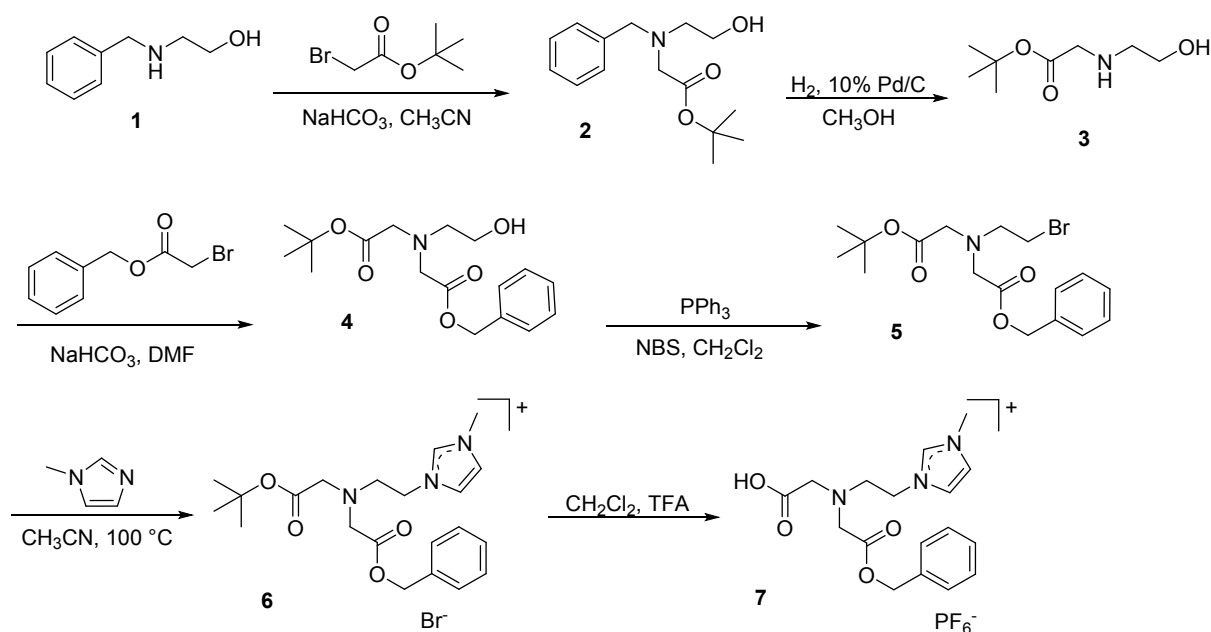
Result and Discussion

Ligand synthesis

A key goal of this work was the development of bifunctional tridentate *N*-heterocyclic carbene pro-ligands that would form neutral complexes of the $[\text{Re}(\text{CO})_3]^+$ core. To this end, the closely related pro-ligands **7** (Scheme 1) and **10** (Scheme 3) were prepared. The synthetic pathway for the formation of pro-ligand **7** began with the reductive amination of benzaldehyde with ethanolamine using sodium borohydride (NaBH_4) to produce **1** (Scheme 1). Compound **1** was then *N*-alkylated with *t*-butyl bromoacetate to form **2** followed by removal of the amine benzyl-protecting group via catalytic hydrogenolysis, yielding compound **3**. The deprotected secondary amine of **3** was then *N*-alkylated with benzyl bromoacetate to form **4**, thereby introducing orthogonal *t*-butyl ester and benzyl ester carboxylic acid protecting groups. The orthogonal protecting groups were introduced to allow selective deprotection using either trifluoroacetic acid (TFA) or via catalytic hydrogenolysis. The primary alcohol unit of **4** was then converted to an alkyl bromide using triphenylphosphine and *N*-bromosuccinimide to produce compound **5** and the alkylation of 1-methylimidazole with **5** produced the imidazolium salt **6** (Scheme 1). Removal of the *t*-butyl ester group of **6** with TFA yielded compound **7** with a free carboxylic acid group. Difficulties were encountered in the purification of **7** as the bromide salt and to overcome this issue, a metathesis reaction was performed to convert the bromide anion to hexafluorophosphate. Thus, **7** was isolated in its pure form as the hexafluorophosphate

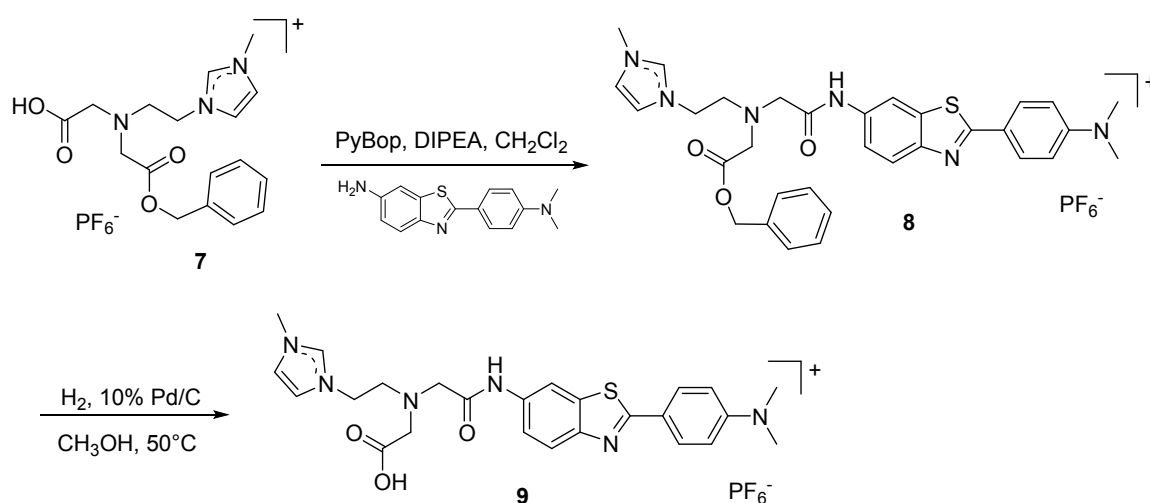
salt, which displayed appropriate solubility in organic solvents for the coupling reaction (amide bond formation) to introduce the amyloid binding moiety.

View Article Online
DOI: 10.1039/C9DT04687A



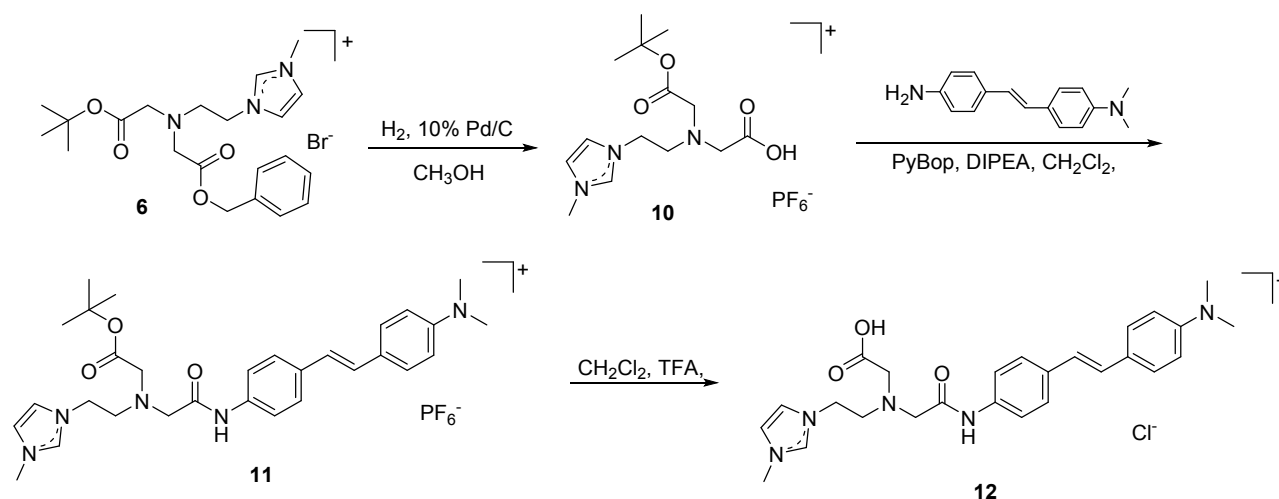
Scheme 1. Synthesis of pro-ligand **7** using the orthogonal protecting group strategy.

The coupling reagent PyBop ((benzotriazol-1-yloxy)tripyrrolidinophosphonium hexafluorophosphate) was used to couple the carboxylic acid group of the pro-ligand **7** and the amine unit of the amyloid binding moiety 6-amino-2-(4-*N,N*-dimethylaminophenyl)benzothiazole (Scheme 2). PyBop was chosen for this reaction as the by-product phosphonium salt could be readily removed from the product **8**, by washing with diethyl ether and the final ligand **9** was obtained as a bright yellow solid after catalytic hydrogenolysis to remove the benzyl ester protecting group (Scheme 2).



Scheme 2. Synthetic scheme for the formation of **9**.

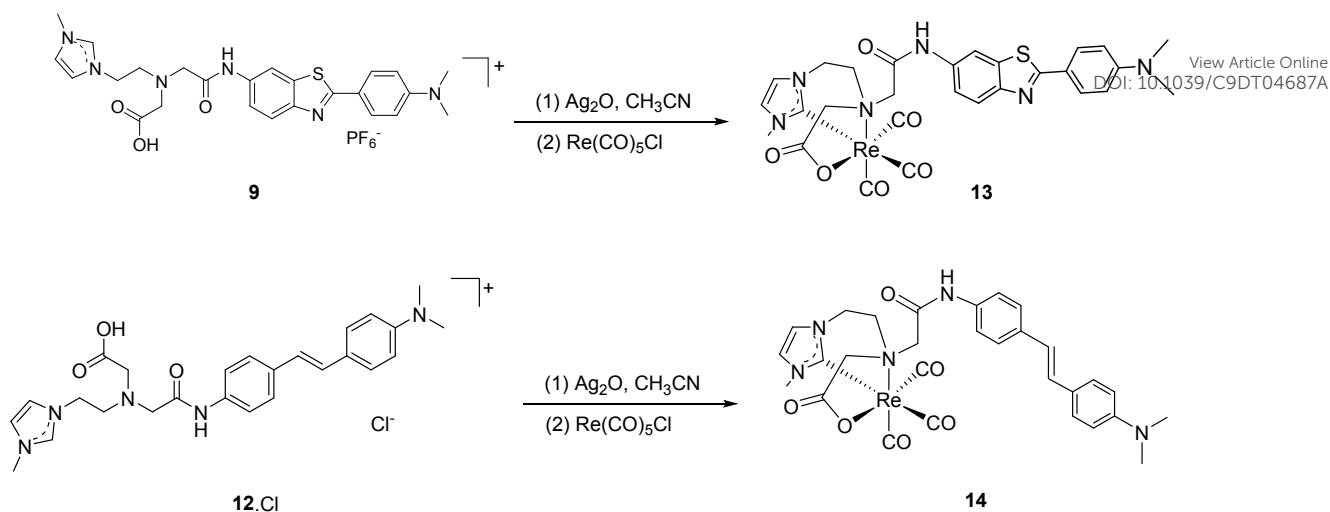
In the case of pro-ligand **12**, coupled to the stilbene-based amyloid binding moiety 4-amino-4'-(*N,N*-dimethylamino)stilbene (Scheme 3), catalytic hydrogenolysis was not suitable for unmasking the final carboxylic acid group due to the potential for simultaneous reduction of the alkene group of the stilbene unit. Therefore, the benzyl ester protecting group of **6** was first deprotected via catalytic hydrogenolysis to generate **10** and the formed carboxylic acid group was then coupled to 4-amino-4'-(*N,N*-dimethylamino)stilbene using PyBop yielding **11** (Scheme 3). The *t*-butyl ester group was then removed in the final step using TFA producing pro-ligand **12**.



Scheme 3. Synthetic pathway for the formation of the stilbene derivative **12**.

Rhenium complex synthesis

A silver transmetalation protocol was utilised for the synthesis of rhenium tricarbonyl complexes **13** and **14** from ligands **9** and **12** respectively (Scheme 4). The silver transmetalation methodology utilising Ag_2O has been commonly employed for the formation of metal complexes of NHC ligands from precursor imidazolium salts,^{23, 24} and we have previously described the synthesis of a range of NHC complexes of the $\text{Re}(\text{CO})_3$ core using this approach.^{16, 17, 21} In the present work, complex **13** was prepared by stirring a suspension of **9** and Ag_2O in acetonitrile for 24 h to allow the Ag -NHC complex to form and then $\text{Re}(\text{CO})_5\text{Cl}$ was added and the reaction mixture was stirred for a further 24 h at 60 °C. After completion of the reaction, the desired complex was purified by column chromatography on alumina and complex **13** was obtained as an orange solid (Scheme 4).



Scheme 4. Synthetic pathway for the formation of the Re complexes **13** and **14**.

For the synthesis of the Re complex of pro-ligand **12**, the same procedure as that described for the preparation of **13** was initially investigated, however the desired compound could not be isolated under these conditions, possibly due to slow formation of the intermediate Ag complex. To facilitate formation of the Ag complex, a metathesis reaction was used to exchange the counterion of **12** from hexafluorophosphate to chloride yielding compound **12·Cl** which allowed for the successful synthesis of the desired Re complex **14** (Scheme 4).

As expected, no signals corresponding to the carboxylic acid or the imidazolium C2 protons of the pro-ligands were apparent in the $^1\text{H-NMR}$ spectra of complexes **13** and **14**, indicating that these groups are deprotonated and coordinated to the Re metal centre. The amide N-H signals resonate as downfield shifted singlets at 10.5 ppm and 10.3 ppm for **13** and **14** respectively (Figures S17 and S18, ESI). The labelled $^1\text{H-NMR}$ spectrum for **13** is shown in Figure 3. As the facially coordinated tridentate ligands have three different donor groups (amine, carboxylate, and carbene) the Re metal is a chiral centre for complexes **13** and **14**, and the non-superimposable mirror image forms of core structure for these complexes are shown in Figure 4. As a result of this chirality, the methylene protons of the acetamide linker group (shown in red on Figure 4) are diastereotopic and resonate as an AB pattern (highlighted in red in Figure 3). The $^{13}\text{C-NMR}$ spectra of complexes **13** and **14** show the expected number of peaks for the respective complexes (Figures S17 and S18, ESI). For each complex, three individual signals corresponding to the carbonyl ligands are evident in the region of 198-196 ppm consistent with this group being *trans* to the three different donor groups of the tridentate ligand.

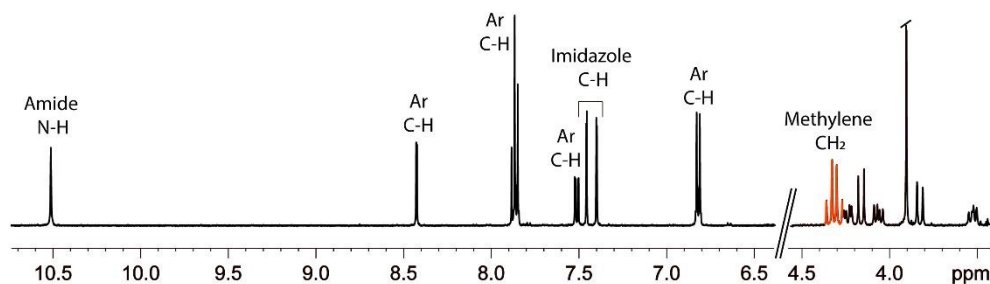


Figure 3. $^1\text{H-NMR}$ spectrum of complex **13** ($\text{DMSO-}d_6$). The signal corresponding to the methylene group protons of the acetamide linker is highlighted in red.

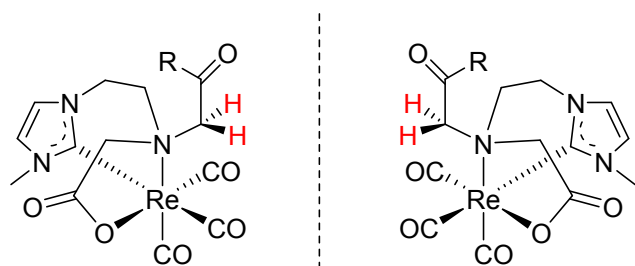


Figure 4. Diagram showing the non-superimposable forms of the chiral complexes **13** and **14** (R = amyloid binding moiety).

To explore the influence of the tridentate ligand on the carbonyl ligands, the solid-state IR spectra for complexes **13** and **14** (Figures S19 and S20, ESI) were recorded. In each case, strong and distinct CO stretching signals were observed at 2017 cm^{-1} and 2015 cm^{-1} , while broad (apparently overlapping as a result of solid-state effects²⁵⁻²⁷) signals were observed at 1890 cm^{-1} and 1886 cm^{-1} for complexes **13** and **14**. These results are consistent with the expected three individual signals for each of the carbonyl ligands which are either *trans* to the amine, carboxylate or carbene donor groups. It is well known that the strong σ -donor properties of NHCs causes the signal for carbonyl ligand *trans* to these groups to be shifted to higher wavenumbers and as such the signals observed at 2017 cm^{-1} and 2015 cm^{-1} for **13** and **14** respectively can be assigned to the carbonyl ligand *trans* to the NHC donor.²⁸

X-ray Structural Studies

The X-ray crystal structure for complex **14** and a poor-quality structure for **13** (included for comparative purposes) are shown in Figure 5. The X-ray crystallographic data for these compounds are given in Table S1 (ESI). In each case, the X-ray crystal structures confirm that the ligands are coordinated to the Re metal centres as *facial* tridentates via the NHC, tertiary amine and carboxylate groups, with the additional three coordination sites being occupied by carbonyl ligands. For

compounds **13** and **14** respectively, the benzothiazole- and stilbene-based amyloid binding moieties are linked to the tertiary amine donor atom via an acetamide linkage. The Re–C_{carbene}, Re–N_{amine} and Re–O_{carboxylate} bond lengths (Figure 5 caption) are similar for each complex and the Re–C_{carbonyl} bond lengths lie within typical ranges (1.90–2.10 Å).^{18, 27, 29} As mentioned in the previous section, NHC ligands are strong σ -donors and are well known to exert a strong *trans* influence. In the case of compound **14**, the *trans* influence exerted by the NHC ligand is apparent and the Re–carbonyl bond length (Re–C(2) = 1.962(7) Å) is significantly longer than those for the two other carbonyl ligands (Re–C(3) = 1.928(8) Å and Re–C(4) = 1.916(8) Å). In contrast, this effect is not observed in the structure for **13**, however this is possibly a result of the lower quality of this structure.

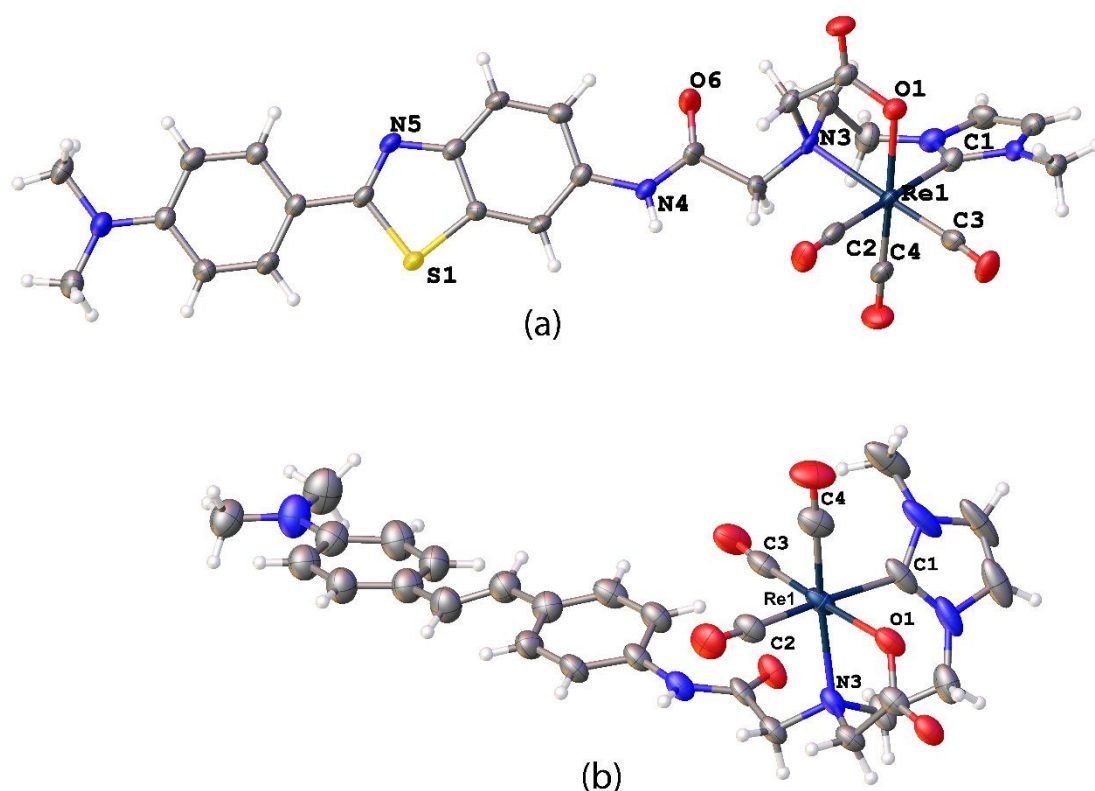


Figure 5. X-ray crystal structures of the Re complexes (a) **13** and (b) **14**. Ellipsoids are shown 40% probability. Selected bond lengths: **13** Re–O(1) = 2.124(19) Å, Re–N(3) = 2.30(2) Å, Re–C(1) = 2.22(3) Å, Re–C(2) = 1.90(4) Å, Re–C(3) = 1.91(3) Å, Re–C(4) = 1.90(3) Å and **14** Re–O(1) = 2.156(4) Å, Re–N(3) = 2.273(5) Å, Re–C(1) = 2.164(7) Å, Re–C(2) = 1.962(7) Å, Re–C(3) = 1.928(8) Å, Re–C(4) = 1.916(8) Å.

Octanol-Water Partition Coefficient

The NHC ligand reported here were designed for the generation of neutral complexes with either the [Re(CO)₃]⁺ or [Tc(CO)₃]⁺ cores for potential radiopharmaceutical applications. As neuroimaging applications are of interest, neutral complexes were desired to achieve sufficient

lipophilicity to modulate the blood brain barrier (BBB) permeability. Molecules are known to cross the blood-brain barrier (BBB) by several mechanisms, including passive diffusion or active transport. Passive diffusion is the most common mechanism for drugs to cross the BBB and relies upon a moderate to high degree of lipid solubility.³⁰ To evaluate the lipid solubility of the Re complexes **13** and **14**, the $\log P$ values were estimated using octanol-water partition coefficient experiments, conducted using the slow stirring method.³¹ The results of these studies shown that complex **13** has $\log P$ value of 0.15 ± 0.01 , while complex **14** has a higher $\log P$ value of 0.39 ± 0.01 . These $\log P$ values of both are somewhat lower than the optimum range required for good BBB permeability, for example Hansch and Leo found that BBB penetration is optimal when the $\log P$ values are in the range of 1.5-2.7.³² However, with the development of this new synthetic approach for the preparation of tridentate NHC pro-ligands, the introduction of more lipophilic groups (for example extended alkyl chains on the NHC units) will be straightforward and allow for the ready modulation of $\log P$ values for the resulting complexes.

Interaction of **13** and **14** with Amyloid- β (1-40) and Amyloid-Plaques

The formation of amyloid- β (A β) fibrils from the A β ₍₁₋₄₀₎ peptide *in vitro* can be monitored using thioflavin-T (ThT) as the interaction between ThT and A β fibrils results in strong fluorescence emission at 480 nm.³³⁻³⁸ The interaction between the Re complexes **13** and **14** and amyloid was studied using a ThT-based fluorescence assay. The fluorescence emission at $\lambda_{em} = 480$ nm for a freshly prepared solution of A β ₁₋₄₀ (4 μ M) and ThT (4 μ M) at 37 °C in the presence of each of the complexes **13** and **14** was monitored over a period of 66 h but no change was observed after 10 h (Figure 6). The control sample, where no complex was added, confirmed the formation of A β fibrils as indicated by the increased fluorescence intensity for fibril-bound ThT at $\lambda_{em} = 480$ nm. The addition of either complex **13** or **14** resulted in a significantly reduced fluorescence suggesting that Re complexes **13** and **14** either bind competitively with ThT to A β ₍₁₋₄₀₎ fibrils or that the complexes inhibit the formation of A β ₍₁₋₄₀₎ fibrils.

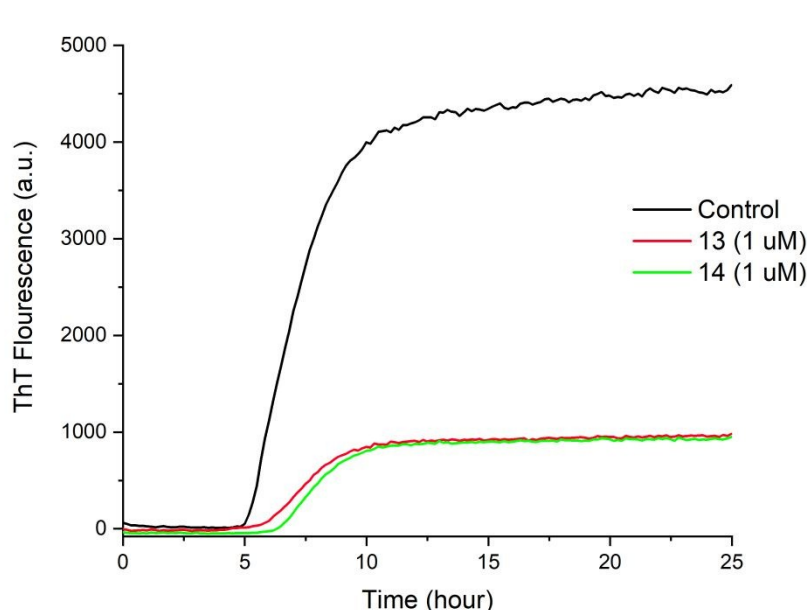


Figure 6. Thioflavin T (ThT) fluorescence assay over a period of 25 h for solutions of ThT (4 μM) and $\text{A}\beta_{1-40}$ (4 μM) at 37 $^{\circ}\text{C}$ in the presence of: no addition (control, black), **13** (red) and **14** (green) (1 μM in each case).

The capacities of the complexes to bind to amyloid plaques in human brain tissue were investigated using epi-fluorescence microscopy. To facilitate these studies the electronic absorption and emission spectra for the metal complexes **13** and **14** (together with the pro-ligands **9** and **12**) were recorded (Figures S23-S26, ESI) and for the complexes, the emission maxima occurred at $\lambda \sim 420$ nm and $\lambda \sim 457$ nm respectively. Frontal cortex brain tissue (7 μm sections) collected from post-mortem subjects with clinically diagnosed AD was compared to tissue from an age-matched healthy control following treatment with complex **13** or complex **14**. The treated tissues were examined by epi-fluorescence microscopy and then compared to contiguous sections that were immuno-stained with an anti-amyloid- $\beta_{(1-42)}$ antibody (1E8) to identify $\text{A}\beta$ plaques (Figure 7). The results of these human brain staining studies showed evidence for moderate levels of co-localisation of complexes **13** and **14** with the amyloid- β plaques (Figure 7b and 7f). However, the epi-fluorescent images for the age-matched controls showed no evidence of non-specific binding for both complexes. Although the cause of the relatively low levels of co-localisation for these complexes with the amyloid plaques is not known, it may be due to the relatively short linker group between the amyloid binding moiety and the relatively large octahedral Re metal complexes.

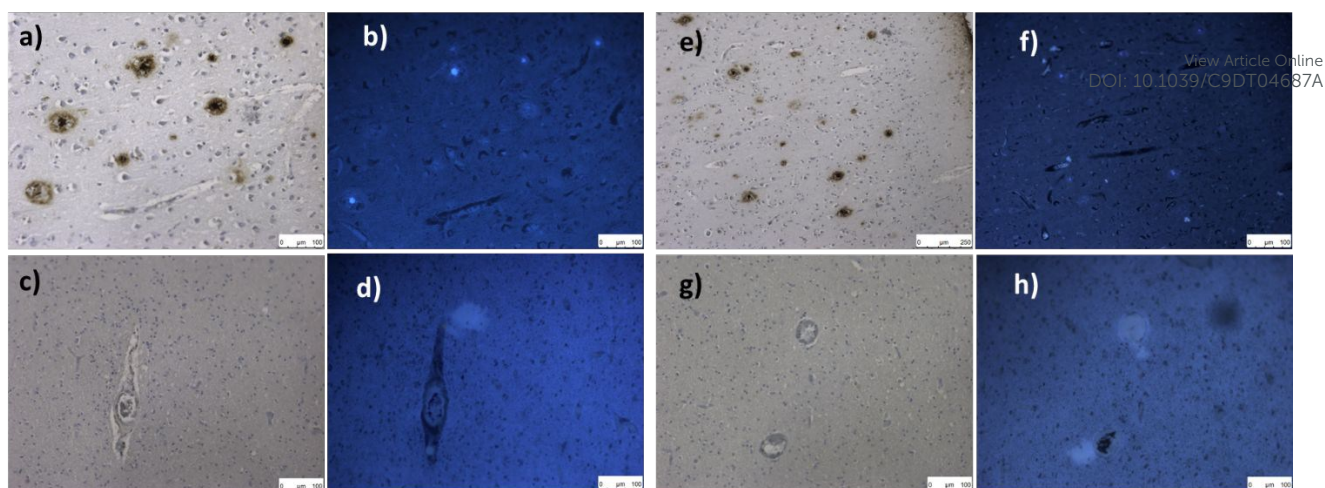


Figure 7. Epi-fluorescence microscopy images of frontal cortex brain tissue from AD patient treated (a, b, e & f) and from healthy age-matched control (c, d, g & h). Images a, e, c & g were stained with amyloid specific antibody (1E8) and visualised under brightfield. Images b & d were stained with **13** and f & h were stained with **14** and visualised using epi-fluorescence microscopy ($\lambda_{\text{ex}} = 405 \text{ nm}$, $\lambda_{\text{em}} = 460 \text{ nm}$)

Conclusion

In conclusion, two tridentate *N*-heterocyclic carbene pro-ligands bearing imidazolium, amine and carboxylate donor groups coupled to either a benzothiazole- or a stilbene-based amyloid binding moiety were designed and synthesised. These pro-ligands were then used to prepare two neutral NHC complexes of the $[\text{Re}(\text{CO})_3]^+$ core (**13** and **14**) and the $\log P$ values for these compounds were determined to be 0.15 ± 0.01 and 0.39 ± 0.01 respectively. Studies using the histological dye Thioflavin-T showed that these complexes bound to fibrils formed from the amyloid- $\beta_{(1-40)}$ peptide. Epi-fluorescence microscopy co-localisation studies for compounds **13** and **14** and the amyloid specific antibody 1E8 in frontal cortex brain tissue from AD patient were consistent with the complexes binding to amyloid- β plaques at moderate to low levels. It is possible that the presence of the octahedral metal complex and the relatively low lipophilicity of **13** and **14** reduced their ability to bind to amyloid plaques. The new ligand systems reported here are promising for the development of NHC based imaging agents as they form neutral and stable complexes with the $[\text{Re}(\text{CO})_3]^+$ core. The $\log P$ values for the Re complexes (**13** and **14**) are not within the optimum range for CNS penetration, however the structures of the synthesised pro-ligands offer the potential to be modified to increase the lipophilicity. For example, the NHC unit has a methyl substituent and this could be modified to a more lipophilic component e.g. *tert*-butyl or cyclohexyl in a relatively straightforward manner. Currently we are undertaking studies into the preparation of the corresponding $^{99\text{m}}\text{Tc}(\text{CO})_3$ complexes of these ligands and these results will be communicated in due course.

Experimental details

General procedures: All reagents were purchased from Sigma Aldrich or Alfa Aesar and were used without further purification unless otherwise stated. 6-amino-2-(4-*N,N*-dimethylaminophenyl)benzothiazole³⁹ and 4-amino-4'-(*N,N*-dimethylamino)stilbene^{29, 40} were synthesised as described previously. NMR spectra were recorded on either a Bruker Avance ARX-400 (400.13 MHz for ¹H, 100.61 MHz for ¹³C), or a Bruker Avance ARX-500 (500.13 MHz for ¹H, 125.77 MHz for ¹³C) spectrometer and were internally referenced to solvent resonances. High resolution mass spectra were obtained using an Agilent 6530 QTOF LC/MS mass spectrometer fitted with an Agilent electrospray ion (ESI) source. UV-visible spectra were recorded using an Agilent Technologies Cary 300 UV-visible spectrophotometer using quartz cuvettes (1 cm). Fluorescence spectra were recorded on a Varian Cary Eclipse spectrofluorimeter (5 nm bandpass, 1 nm data interval, PMT voltage: 600 V) using quartz cuvettes (1 cm). Infra-red spectra were recorded using an Agilent Cary 660 FT-IR spectrophotometer in ATR mode.

X-ray Crystallography. Single crystals of complexes **13** and **14** suitable for X-ray diffraction studies were grown by slow evaporation in dichloromethane solutions of these complexes. Crystallographic data for all structures determined are given in Table S1 (Supporting Information). For all samples, crystals were removed from the crystallisation vial and immediately coated with Paratone oil on a glass slide. A suitable crystal was mounted in Paratone oil on a glass fiber and cooled rapidly to 150K (**13**) or 136K (**14**) in a stream of cold N₂ using an Oxford low-temperature device. Diffraction data were measured using an Oxford Gemini diffractometer mounted with Mo-K α λ = 0.71073 Å and Cu-K α λ = 1.54184 Å. Data were reduced and corrected for absorption using the CrysAlis Pro program.⁴¹ The SHELXL2013-2⁴² program was used to solve the structures with Direct Methods, with refinement by the Full-Matrix Least-Squares refinement techniques on F^2 . The non-hydrogen atoms were refined anisotropically and hydrogen atoms were placed geometrically and refined using the riding model. Coordinates and anisotropic thermal parameters of all non-hydrogen atoms were refined. All calculations were carried out using the program Olex^{2,43} Further XRD details are provided in the Electronic Supplementary Information. CCDC 1969630-1969631 contains the supplementary crystallographic data for this paper. These data can be obtained free of charge from The Cambridge Crystallographic Data Centre via <https://www.ccdc.cam.ac.uk/structures/>

ThT Fluorescence A β binding Assays. Synthetic A β ₁₋₄₀ (500 μ g, Bachem, 4014442) was dissolved in HFIP (500 μ L) then incubated on ice for 1 hour. The solution was then allowed to evaporate overnight followed by drying by high speed vacuum centrifugation to remove residual HFIP and moisture. The peptide was dissolved in 60 mM NaOH (100 μ L) and incubated for 3 min at room

temperature then MilliQ water (350 μL) was added and the solution was vortex briefly followed by ultrasonication for 5 minutes on ice. $10 \times$ PBS (pH 7.4, 50 μL) was added to the solution then vortexed briefly and centrifuged for 5 min. Supernatant was transferred to a fresh tube and kept on ice. The concentration of the $\text{A}\beta_{1-40}$ solution was determined by its absorbance at 214 nm ($\epsilon = 94526 \text{ M}^{-1} \text{ cm}^{-1}$) and found to be 148 μM . Stock solutions of ThT (1 mM in PBS), complexes **13** and **14** (1 mM in DMSO) were prepared freshly and final samples were prepared on ice by mixing $\text{A}\beta_{1-40}$ (final concentration: 4 μM), ThT (final concentration, 4 μM) and the chosen Re complex (final concentration: 1 μM), and the control consisting of $\text{A}\beta_{1-40}$ (final concentration: 4 μM) and ThT (final concentration: 4 μM). All samples were prepared in triplicates and the ThT fluorescence intensity of each sample was recorded every 10 min at 37 $^{\circ}\text{C}$ using a FLUOstar Omega filter-based multi-mode microplate reader with 440/480 nm excitation/emission filters over a period of 66 h with orbital shaking before each cycle.

Staining of Human AD Brain Tissues. The Health Sciences Human Ethics Sub-committee, The University of Melbourne, approved all experiments using human brain tissue (Ethics Approval No. 1341145). Brain tissue was collected at autopsy. Brain tissue from the frontal cortex was preserved by formalin fixation and paraffin embedding. AD pathology was confirmed according to standard National Institute of Aging and Reagan Institute Working Group on Diagnostic Criteria for the Neuropathological Assessment of Alzheimer's Disease (1997) criteria. The brain tissue samples of age-matched Human controls (HC) were subject to the above criteria. The AD and HC brain tissue sections (7 μm) were first deparaffined (xylene, 3×2 min) followed by rehydration (soaking for 2 min in a series of 100%, 90%, 70%, and 0% v/v ethanol/water). The hydrated tissue sections were washed in phosphate buffer saline (PBS, 5 min). Autofluorescence of the tissue was quenched using potassium permanganate (KMnO_4) (0.25% in PBS, 20 min) and the sections were further washed with PBS (2×2 min) to remove the excess KMnO_4 . The brown-coloured sections were washed with potassium metabisulfite and oxalic acid (1% in PBS) until the brown colour was removed followed by washing with PBS (3×2 min). The sections were blocked with bovine serum albumin (2% BSA in PBS, pH 7.0, 10 min) and covered with a solution of the chosen Re complex (10 μM in 15% v/v DMSO/PBS, 10 min). The sections were treated with BSA again (4 min) to remove any Re complex non-specifically bound to the tissue. Finally, the sections were washed with PBS (3×2 min), DI water, and mounted with a DAKO fluorescence mounting medium. Fluorescence images were visualized using a Leica DM IL LED microscope.

Partition coefficient (LogP) studies. 1-Octanol/water partition coefficients for complexes **13** and **14** were determined using the slow-stirring method as described by Pereiro and co-workers.³¹ The 1-octanol and Milli-Q water were saturated prior their use and the starting concentration of complexes

13 and **14** in the 1-octanol phase was 80 μM . Approximately 5 mL of the pre-saturated water and 1-octanol were added to a glass vial containing a magnetic stir bar. The vials were slowly stirred and maintained at 25 $^{\circ}\text{C}$ for two days. The metal complex concentration in the 1-octanol phase was then analysed using an Agilent Technologies Cary 300 UV-visible spectrophotometer in a quartz cuvette (1 cm). A calibration curve for each complex was prepared at its λ_{max} value (365 nm for **13** and 360 nm for **14**).

Synthesis

6: A solution of 1-methylimidazole (0.12 g, 1.51 mmol) in acetonitrile (10 mL) was added dropwise to a solution of **5** (0.58 g, 1.51 mmol) in acetonitrile (40 mL) and the mixture was refluxed at 100 $^{\circ}\text{C}$ overnight. After removal of solvent on a rotatory evaporator, the crude product was purified on silica with methanol (2%) and dichloromethane (98%) as the eluent and the pure product was obtained as a yellow oil. (Yield: 0.47 g, 81%). ^1H NMR (400 MHz) (CDCl_3): δ (ppm) 1.42 (s, 9H, CH_3), 3.18 (m, 2H, CH_2), 3.39 (s, 2H, CH_2), 3.56 (s, 2H, CH_2), 3.99 (s, 3H, $\text{CH}_{3\text{imi}}$), 4.43 (m, 2H, CH_2), 7.26 (t, 1H, $^3J_{\text{H-H}} = 1.76$ Hz, H_{imi}), 7.31-7.36 (m, 5H, H_{Ar}), 7.88 (t, 1H, $^3J_{\text{H-H}} = 1.72$ Hz, H_{imi}), 10.0 (s, 1H, NCHN). ^{13}C NMR (CDCl_3): δ (ppm) 36.5 $\text{CH}_{3\text{imi}}$, 48.2 CH_2 , 50.6 C_q , 55.0 NCH_2 , 56.1 NCH_2 , 56.7 NCH_2 , 66.7 O $\text{CH}_2\text{-Ar}$, 81.9 C_q , 122.0 C_{imi} , 123.6 C_{imi} , 128.3 C_{Ar} , 128.5 C_{Ar} , 128.7 C_{Ar} , 135.3 C_q , 138.0 C_{imi} , 170.3 C_q , 171.1 C_q . HRESI- MS^+ (CH_3OH): $[\text{C}_{21}\text{H}_{30}\text{N}_3\text{O}_4]^+$ $m/z = 388.2257$, calcd = 388.2236.

7: To a stirred solution of **6** (0.40 g, 1.03 mmol) in dichloromethane (15 mL) at 0 $^{\circ}\text{C}$ was added dropwise a solution of trifluoroacetic acid (2.55 g, 22.3 mmol) in dichloromethane (5 mL). The mixture was then stirred at room temperature overnight. After removal of the solvent on a rotatory evaporator, a yellow oil was obtained, which was dissolved in water (20 mL) and a saturated solution of KPF_6 (1.33 g, 7.22 mmol) in water (20 mL) was added dropwise resulting in the formation of a white precipitate. The mixture was extracted with dichloromethane (3×20 mL) and the combined organic extracts were dried with MgSO_4 . The solvent was removed on a rotatory evaporator yielding the pure compound as a colourless oil. (Yield: 0.47 g, 44%). ^1H NMR (500 MHz) ($\text{DMSO-}d_6$): δ (ppm) 3.05 (t, 2H, $^3J_{\text{H-H}} = 5.48$ Hz, CH_2), 3.45 (s, 2H, NCH_2), 3.61 (s, 2H, NCH_2), 3.81 (s, 3H, CH_3), 4.21 (t, 2H, CH_2), 5.10 (s, 2H, $\text{CH}_{2\text{benzyl}}$), 7.34-7.39 (m, 5H, H_{Ar}), 7.63 (t, 1H, $^3J_{\text{H-H}} = 1.64$ Hz, H_{imi}), 7.71 (t, 1H, $^3J_{\text{H-H}} = 1.68$ Hz, H_{imi}), 9.05 (s, 1H, NCHN_{imi}). ^{13}C NMR ($\text{DMSO-}d_6$): δ (ppm) 36.1 CH_3 , 47.6 CH_2 , 53.9 CH_2 , 54.0 NCH_2 , 55.0 NCH_2 , 66.1 O- $\text{CH}_2\text{-Ar}$, 123.2 C_{imi} , 123.3 C_{imi} , 128.5 C_{Ar} , 128.6 C_{Ar} , 128.9 C_{Ar} , 136.4 C_q , 137.5 C_{imi} , 171.4 $\text{C}=\text{O}$, 172.9 $\text{C}=\text{O}$. HRESI- MS^+ (CH_3OH): $[\text{C}_{17}\text{H}_{22}\text{N}_3\text{O}_4]^+$ $m/z = 332.1607$, calcd = 332.1610.

8: A mixture of **7** (0.32 g, 0.67 mmol), DIPEA (0.24 g, 1.83 mmol), PyBop (0.32 g, 0.670 mmol) and 6-amino-2-(4-*N,N*-dimethylaminophenyl)benzothiazole (0.16 g, 0.670 mmol) in dichloromethane (20 mL) was stirred at room temperature overnight. The solvent was removed using a rotary evaporator and the crude product was washed with diethyl ether (3 × 10 mL) and a minimal amount of dichloromethane to yield the pure product as a yellow solid. (Yield: 0.26 g, 40%). ¹H NMR (400 MHz) (DMSO-*d*₆): δ (ppm) 3.02 (s, 6H, CH₃), 3.17 (t, 2H, ³J_{H-H} = 5.16 Hz, CH₂), 3.57 (s, 2H, NCH₂O), 3.72 (s, 2H, NCH₂), 3.76 (s, 3H, CH₃_{imi}), 4.28 (t, 2H, ³J_{H-H} = 5.28 Hz, CH₂), 5.15 (s, 2H, CH₂), 6.82 (d, 2H, ³J_{H-H} = 9.00 Hz, H_{Ar}), 7.34-7.39 (m, 5H, H_{Ar}), 7.61 (s, 1H, H_{Ar}), 7.78 (d, 1H, ³J_{H-H} = 1.56 Hz, H_{imi}), 7.84-7.87 (m, 3H, H_{Ar}), 8.36 (d, 1H, ³J_{H-H} = 1.92 Hz, H_{imi}), 9.12 (s, 1H, H_{imi}), 9.91 (s, 1H, NH). ¹³C NMR (DMSO-*d*₆): δ (ppm) 36.1 CH₃_{imi}, 39.5-40.5 CH₃, 47.6 CH₂, 54.4 CH₂, 55.5 NCH₂, 58.3 NCH₂, 66.2 O-CH₂-Ar, 111.9 C_{imi}, 112.3 C_{Ar}, 119.0 C_q, 120.7 C_{Ar}, 122.3 C_{Ar}, 123.2 C_{imi}, 123.5 C_{Ar}, 128.5-128.9 C_{benzothiazole}, 134.8 C_q, 135.9 C_q, 136.3 C_q, 137.5 C_{imi}, 150.6 C_q, 152.6 C_q, 167.1 C_q, 169.6 C_q, 171.8 C_q. HRESI-MS⁺ (CH₃OH): [C₃₂H₃₅N₆O₃S]⁺ *m/z* = 583.2516, calcd = 583.2491.

9: To a solution of **8** (0.21 g, 0.30 mmol) in hot methanol (50 mL) was added 10% Pd/C (0.05 g) and the mixture was heated at 40 °C under an atmosphere of hydrogen for 5 h. The reaction mixture was filtrated through a plug of Celite, and after removal of the solvent on a rotatory evaporator the product was obtained as a bright yellow solid. (Yield: 0.18 g, 82%). ¹H NMR (400 MHz) (DMSO-*d*₆): δ (ppm) 3.02 (s, 6H, CH₃), 3.16 (t, 2H, ³J_{H-H} = 5.48, NCH₂), 3.54 (s, 2H, NCH₂), 3.54 (s, 2H, NCH₂), 3.77 (s, 3H, NCH₃), 4.26 (t, 2H, ³J_{H-H} = 5.36, CH₂), 6.82 (d, 2H, ³J_{H-H} = 8.92, H_{Ar}), 7.45-7.47 (dd, 1H, H_{Ar}), 7.62 (s, 1H, H_{Ar}), 7.79 (s, 1H, H_{imi}), 7.85 (d, 2H, H_{Ar}), 7.87 (d, 1H, H_{Ar}), 8.37 (d, 1H, ³J_{H-H} = 1.80 Hz, H_{imi}), 9.14 (s, 1H, H_{imi}). ¹³C NMR (DMSO-*d*₆): δ (ppm) 36.1 CH₃_{imi}, 39.5-40.5 CH₃, 47.6 CH₂, 55.7 NCH₂, 58.6 NCH₂, 111.8 C_{imi}, 112.3 C_{Ar}, 118.9 C_{Ar}, 120.7 C_q, 122.3 C_{Ar}, 123.2 C_{imi}, 123.5 C_{Ar}, 128.7 C_{Ar}, 134.9 C_q, 135.9 C_q, 137.5 C_{imi}, 150.5 C_q, 152.6 C_q, 167.1 C_q, 169.9 C_q, 173.7 C_q. HRESI-MS⁺ (CH₃OH): [C₂₅H₂₉N₆O₃S]⁺ *m/z* = 493.1995, calcd = 493.2022.

10: To a stirred solution of **6** (5.50 g, 11.7 mmol) in methanol (70 mL), 10% Pd/C (0.50 g) was added and the reaction was stirred under an atmosphere of hydrogen overnight. The mixture was filtered through a plug of Celite and the solvent was removed on a rotatory evaporator yielding a yellow oil. The yellow oil was dissolved in water (10 mL) and a solution of KPF₆ (1.01 g, 5.51 mmol) in water (10 mL) was added dropwise, resulting in the formation of a white precipitate. The mixture was extracted with dichloromethane (3 × 10 mL) and the combined organic extracts were dried with MgSO₄ and the solvent was removed on a rotatory evaporator yielding the pure compound as yellow

oil. (Yield: 0.45 g, 38%). ^1H NMR (400 MHz) ($\text{DMSO-}d_6$): δ (ppm) 1.40 (s, 9H, CH_3), 3.03 (t, 2H, $^3J_{\text{H-H}} = 5.64$ Hz, CH_2), 3.41 (s, 2H, NCH_2), 3.43 (s, 2H, NCH_2), 4.21 (t, 2H, $^3J_{\text{H-H}} = 5.36$ Hz, CH_2), 7.67 (s, 1H, H_{imi}), 7.75 (s, 1H, H_{imi}), 9.08 (s, 1H, H_{imi}). ^{13}C NMR ($\text{DMSO-}d_6$): δ (ppm) 28.3 CH_3 , 36.1 $\text{CH}_{3\text{imi}}$, 47.6 CH_2 , 54.0 CH_2 , 55.0 NCH_2 , 55.8 NCH_2 , 80.9 C_q , 123.2 C_{imi} , 123.2 C_{imi} , 137.5 C_{imi} , 170.7 $\text{C}=\text{O}$, 172.9 $\text{C}=\text{O}$. HRESI- MS^+ (CH_3OH): $[\text{C}_{14}\text{H}_{24}\text{N}_3\text{O}_4]^+ m/z = 298.1766$, calcd = 298.1767.

11: The compound was prepared as described for **9** from **10** (0.20 g, 0.43 mmol), DIPEA (0.17 g, 1.30 mmol), PyBop (0.23 g, 0.43 mmol), 4-amino-4'-(*N,N*-dimethylamino)stilbene (0.10 g, 0.42 mmol). (Yield: 0.05 g, 17%). ^1H NMR (400 MHz) ($\text{DMSO-}d_6$): δ (ppm) 1.43 (s, 9H, $\text{CH}_{3\text{t-butyl}}$), 2.93 (s, 6H, $\text{CH}_{3\text{stilbene}}$), 3.13 (t, 2H, $^3J_{\text{H-H}} = 5.75$ Hz, CH_2), 3.48 (s, 4H, NCH_2), 3.78 (s, 3H, $\text{CH}_{3\text{imi}}$), 4.25 (t, 2H, $^3J_{\text{H-H}} = 5.70$ Hz, CH_2), 6.71 (d, 2H, $^3J_{\text{H-H}} = 8.85$ Hz, H_{Ar}), 6.91 (d, 1H, $^3J_{\text{H-H}} = 16.4$ Hz, $\text{CH}=\text{CH}$), 7.03 (d, 1H, $^3J_{\text{H-H}} = 16.5$ Hz, $\text{CH}=\text{CH}$), 7.40 (d, 2H, $^3J_{\text{H-H}} = 8.80$ Hz, H_{Ar}), 7.47 (d, 2H, $^3J_{\text{H-H}} = 8.70$ Hz, H_{Ar}), 7.52 (d, 2H, $^3J_{\text{H-H}} = 8.60$ Hz, H_{Ar}), 7.64 (s, 1H, H_{imi}), 7.78 (s, 1H, H_{imi}), 9.10 (s, 1H, H_{imi}), 9.72 (s, 1H, NH). ^{13}C NMR ($\text{DMSO-}d_6$): δ (ppm) 28.3 $\text{CH}_{3\text{t-butyl}}$, 36.1 $\text{CH}_{3\text{imi}}$, 39.5 $\text{CH}_{3\text{stilbene}}$, 47.6 CH_2 , 54.5 CH_2 , 56.4 NCH_2 , 58.3 NCH_2 , 81.3 $\text{C}_{\text{t-butyl}}$, 112.8 C_{Ar} , 119.6 C_{Ar} , 123.2 C_{imi} , 123.5 C_{imi} , 123.6 C_{Ar} , 125.6 C_{Ar} , 126.7 C_{Ar} , 127.8 C_{Ar} , 128.0 C_q , 133.6 C_q , 137.5 C_{imi} , 137.7 C_q , 150.3 C_q , 169.5 $\text{C}=\text{O}$, 171.2 $\text{C}=\text{O}$. HRESI- MS^+ (CH_3OH): $[\text{C}_{30}\text{H}_{40}\text{N}_5\text{O}_3]^+ m/z = 518.3162$, calcd = 518.310.

12: To a stirred solution of **11** (0.28 g, 0.42 mmol) in dichloromethane (15 mL) at 0 $^\circ\text{C}$ was added dropwise a solution of trifluoroacetic acid (2.37 g, 20.8 mmol) in dichloromethane (5 mL) and the mixture was stirred at room temperature overnight. The solvent was removed on a rotatory evaporator yielding a yellow solid, which was dissolved in water (20 mL), the pH was then adjusted to 12 with 1M NaOH and the solution washed with dichloromethane (3×10 mL). The pH of the solution was then adjusted to pH 7 using concentrated hydrochloric acid and the water was removed using rotatory evaporator to obtain a yellow solid. The yellow solid (0.44 g) was redissolved in acetonitrile and a solution of Bu_4NCl (0.26 g, 0.95 mmol) in acetonitrile was added dropwise and the yellow precipitate was collected via centrifugation. The solvent was removed on a rotatory evaporator yielding the pure compound as a yellow solid. (Yield: 0.21 g, 57%). ^1H -NMR (500 MHz) ($\text{DMSO-}d_6$): δ (ppm) 2.92 (s, 6H, $\text{CH}_{3\text{stilbene}}$), 3.11 (t, 2H, $^3J_{\text{H-H}} = 5.50$ Hz, CH_2), 3.16 (s, 4H, CH_2), 3.65 (s, 3H, $\text{CH}_{3\text{imi}}$), 4.21 (s, 2H, CH_2), 6.70 (d, 2H, $^3J_{\text{H-H}} = 9.15$ Hz, H_{Ar}), 6.90 (d, 1H, $^3J_{\text{H-H}} = 16.4$ Hz, $\text{CH}=\text{CH}$), 7.01 (d, 1H, $^3J_{\text{H-H}} = 16.4$ Hz, $\text{CH}=\text{CH}$), 7.39 (d, 2H, $^3J_{\text{H-H}} = 8.80$ Hz, H_{Ar}), 7.44 (d, 2H, $^3J_{\text{H-H}} = 8.60$ Hz, H_{Ar}), 7.54 (s, 1H, H_{imi}), 7.65 (d, 2H, $^3J_{\text{H-H}} = 8.40$ Hz, H_{Ar}), 7.83 (s, 1H, H_{imi}), 9.83 (s, 1H, H_{imi}). ^{13}C NMR ($\text{DMSO-}d_6$): δ (ppm) 35.9 $\text{CH}_{3\text{imi}}$, 39.5 $\text{CH}_{3\text{stilbene}}$, 47.8 CH_2 , 56.4 CH_2 , 58.1 CH_2 , 61.7 CH_2 , 65.4 C_q , 112.8 C_{Ar} , 119.6 C_{Ar} , 123.0 C_{imi} , 123.4 C_{imi} , 123.9 $\text{CH}=\text{CH}$, 125.7 C_q , 126.5 C_{Ar} , 127.6 C_q , 127.7 C_{Ar} ,

133.1 C_q , 138.0 C_{imi} , 150.3 C_q , 171.3 C_q . HRESI-MS⁺ (CH_3OH): $[C_{26}H_{32}N_5O_3]^+$ $m/z = 462.2512$, calcd = 462.2505.

View Article Online
DOI: 10.1039/C9DT04687A

13: A mixture of **9** (0.043 g, 0.069 mmol) and Ag_2O (0.032 g, 0.14 mmol) in acetonitrile (25 mL) was stirred at 60 °C for 24 h. $Re(CO)_5Cl$ (0.025 g, 0.069 mmol) was then added and the mixture was stirred at 60 °C for a further 24 h. The mixture was filtered through Celite and the solvent was removed from the filtrate on a rotatory evaporator yielding a yellow/brown solid. The yellow/brown solid was dissolved in minimal amount of acetonitrile and purified on alumina using methanol (5%) and dichloromethane (95%) as the eluent. The product was obtained as yellow solid. (Yield: 0.020 g, 32%). ¹H-NMR (500 MHz) (DMSO-*d*₆): δ (ppm) 3.02 (s, 6H, CH_3), 3.32-3.33 (m, 1H, CH_2), 3.50-3.55 (m, 1H, CH_2), 3.83 (d, 1H, $^3J_{H-H} = 16.4$ Hz, CH_2COO), 3.90 (s, 3H, CH_{3imi}), 4.04-4.09 (m, 1H, CH_2), 4.16 (d, 1H, $^3J_{H-H} = 16.3$ Hz, CH_2COO), 4.22-4.26 (m, 1H, CH_2), 4.31 (d, 2H, $A^3J_{H-H} = 15.8$ Hz, $B^3J_{H-H} = 15.8$ Hz, CH_2CONH), 6.82 (d, 2H, $^3J_{H-H} = 9.15$ Hz, H_{Ar}), 7.40 (d, 1H, $^3J_{H-H} = 1.75$ Hz, H_{imi}), 7.46 (d, 1H, $^3J_{H-H} = 1.80$ Hz, H_{imi}), 7.51 (dd, 1H, $^3J_{H-H} = 2.15$, 6.65 Hz, H_{Ar}), 7.84-7.88 (m, 3H, H_{Ar}), 8.43 (d, 1H, $^3J_{H-H} = 2.05$, H_{Ar}), 10.5 (s, 1H, NH). ¹³C NMR (DMSO-*d*₆): δ (ppm) 39.0 CH_{3imi} , 39.5-40.5 CH_3 , 47.1 CH_2 , 59.8 CH_2 , 65.1 CH_2 , 69.4 CH_2 , 112.3 C_{imi} , 119.4 C_{Ar} , 122.4 C_{Ar} , 123.1 C_{Ar} , 123.2 C_{imi} , 128.8 C_{Ar} , 134.9 C_q , 135.6 C_q , 150.8 C_q , 152.6 C_q , 162.8 C_q , 166.8 C_q , 167.4 C_q , 178.5 C_q , 180.1 C_q , 196.2 $Re-CO$, 197.4 $Re-CO$, 197.7 $Re-CO$. HRESI-MS⁺ (CH_3OH): $[C_{28}H_{28}N_6O_6ReSNa]^+$ $m/z = 785.1170$, calcd = 785.1168.

14: The compound was prepared as described for **13** from **12** (0.043 g, 0.069 mmol), Ag_2O (0.032 g, 0.14 mmol) and $Re(CO)_5Cl$ (0.025 g, 0.069 mmol) in 1:9 dichloromethane and methanol (25 mL). The product was obtained as yellow solid. (Yield: 0.030 g, 38%). ¹H-NMR (500 MHz) (DMSO-*d*₆): δ (ppm) 2.93 (s, 6H, $CH_{3stilbene}$), 3.32-3.33 (m, 1H, CH_2), 3.46-3.51 (m, 1H, CH_2), 3.80 (d, 1H, $^3J_{H-H} = 16.5$ Hz, CH_2COO), 3.90 (s, 3H, CH_{3imi}), 4.03-4.08 (m, 1H, CH_2), 4.14 (d, 1H, $^3J_{H-H} = 16.0$ Hz, CH_2COO), 4.21-4.24 (m, 1H, CH_2), 4.25-4.31 (m, 2H, CH_2CONH), 6.72 (d, 2H, $^3J_{H-H} = 8.50$ Hz, H_{Ar}), 6.92 (d, 1H, $^3J_{H-H} = 16.0$ Hz, $CH=CH$), 7.05 (d, 1H, $^3J_{H-H} = 16.0$ Hz, $CH=CH$), 7.39-7.41 (m, 3H, H_{Ar}), 7.43 (d, 1H, $^3J_{H-H} = 1.50$ Hz, H_{imi}), 7.49 (d, 2H, $^3J_{H-H} = 9.00$ Hz, H_{Ar}), 7.57 (d, 2H, $^3J_{H-H} = 8.50$ Hz, H_{Ar}), 10.3 (s, 1H, NH). ¹³C NMR (DMSO-*d*₆): δ (ppm) 39.0 CH_{3imi} , 39.5-40.5 $CH_{3stilbene}$, 47.1 CH_2CH_2 , 59.8 CH_2CH_2 , 65.1 CH_2COO , 69.4 CH_2COO , 112.7 C_{Ar} , 120.1 C_{Ar} , 123.1 C_{imi} , 123.2 C_{imi} , 123.6 $CH=CH$, 125.6 C_{Arq} , 126.7 C_{Ar} , 127.8 C_{Ar} , 128.2 $CH=CH$, 134.0 C_{Arq} , 137.4 C_{Arq} , 150.4 C_{Arq} , 166.5 $CONH$, 178.5 COO , 180.2 NCN , 196.2 $Re-CO$, 197.4 $Re-CO$, 197.7 $Re-CO$. HRESI-MS⁺ (CH_3OH): $[C_{29}H_{31}N_5O_6ReNa]^+$ $m/z = 754.1590$, calcd = 754.1651.

Electronic Supplementary Information

Synthesis of 6-nitro-2-(4-*N,N*-dimethylaminophenyl)benzothiazole, 6-amino-2-(4-*N,N*-dimethylaminophenyl)benzothiazole, *p*-nitro-*p*'-*N,N*-dimethylaminostilbene, *p*-amino-*p*'-*N,N*-dimethylaminostilbene and compounds **1-5**. Additional X-ray crystallographic details, UV-vis and emission spectra for **9, 12-14**. Partition coefficient study details and NMR spectra for all prepared compounds. IR spectra for **13** and **14**.

Acknowledgements

We wish to acknowledge the Victorian Brain Bank Network for provision of human brain tissue.

Conflicts of interest

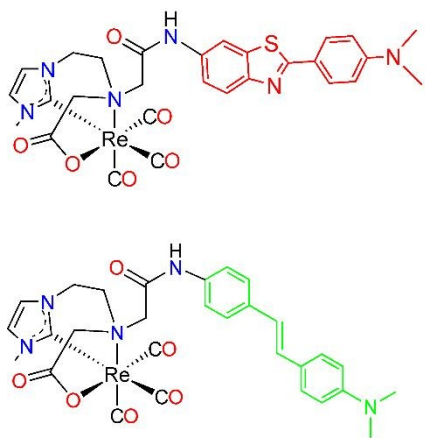
There are no conflicts of interest to declare

Reference

1. G. Moya-Alvarado, N. Gershoni-Emek, E. Perlson and F. C. Bronfman, *Mol. Cell Proteomics*, 2016, **15**, 409-425.
2. M. P. Mattson, *Nature*, 2004, **430**, 631.
3. M. R. Brier, B. Gordon, K. Friedrichsen, J. McCarthy, A. Stern, J. Christensen, C. Owen, P. Aldea, Y. Su, J. Hassenstab, N. J. Cairns, D. M. Holtzman, A. M. Fagan, J. C. Morris, T. L. S. Benzinger and B. M. Ances, *Sci. Transl. Med.*, 2016, **8**, 338ra366-338ra366.
4. S. L. Pimlott and A. Sutherland, *Chem. Soc. Rev.*, 2011, **40**, 149-162.
5. T. J. Wadas, E. H. Wong, G. R. Weisman and C. J. Anderson, *Chem. Rev.*, 2010, **110**, 2858-2902.
6. A. Arora and N. Bhagat, *Int. J. Biomed. Imaging*, 2016, **2016**, 17.
7. M. P. Kung, C. Hou, Z. P. Zhuang, D. Skovronsky and H. F. Kung, *Brain Res.*, 2004, **1025**, 98-105.
8. X. Wang, M. Cui, P. Yu, Z. Li, Y. Yang, H. Jia and B. Liu, *Bioorg. Med. Chem. Lett.*, 2012, **22**, 4327-4331.
9. M. D. Bartholomä, A. S. Louie, J. F. Valliant and J. Zubieta, *Chem. Rev.*, 2010, **110**, 2903-2920.
10. C. Kiritsis, B. Mavroidi, A. Shegani, L. Palamaris, G. Loudos, M. Sagnou, I. Pirmettis, M. Papadopoulou and M. Pelecanou, *ACS Med. Chem. Lett.*, 2017, **8**, 1089-1092.
11. C. J. Chen, K. Bando, H. Ashino, K. Taguchi, H. Shiraishi, K. Shima, O. Fujimoto, C. Kitamura, S. Matsushima, K. Uchida, Y. Nakahara, H. Kasahara, T. Minamizawa, C. Jiang, M. R. Zhang, M. Ono, M. Tokunaga, T. Suhara, M. Higuchi, K. Yamada and B. Ji, *J. Nucl. Med.*, 2015, **56**, 120-126.
12. M. Ono and H. Saji, *Med. Chem. Commun.*, 2015, **6**, 391-402.
13. S. Díez-González, N. Marion and S. P. Nolan, *Chem. Rev.*, 2009, **109**, 3612-3676.
14. R. Visbal and M. C. Gimeno, *Chem. Soc. Rev.*, 2014, **43**, 3551-3574.
15. L. Mercks and M. Albrecht, *Chem. Soc. Rev.*, 2010, **39**, 1903-1912.
16. C. Y. Chan, P. A. Pellegrini, I. Greguric and P. J. Barnard, *Inorg. Chem.*, 2014, **53**, 10862-10873.
17. C. Y. Chan and P. J. Barnard, *Dalton Trans.*, 2015, **44**, 19126-19140.
18. W.-M. Xue, M. C.-W. Chan, Z.-M. Su, K.-K. Cheung, S.-T. Liu and C.-M. Che, *Organometallics*, 1998, **17**, 1622-1630.
19. X.-W. Li, H.-Y. Li, G.-F. Wang, F. Chen, Y.-Z. Li, X.-T. Chen, Y.-X. Zheng and Z.-L. Xue, *Organometallics*, 2012, **31**, 3829-3835.

20. G.-F. Wang, Y.-Z. Liu, X.-T. Chen, Y.-X. Zheng and Z.-L. Xue, *Inorg. Chim. Acta*, 2013, **394**, 488-493.
21. C. Y. Chan, A. Noor, C. A. McLean, P. S. Donnelly and P. J. Barnard, *Chem. Commun.*, 2017, **53**, 2311-2314. View Article Online
DOI: 10.1039/C9DT04687A
22. B. W. Chow and C. Gu, *Trends Neurosci.*, 2015, **38**, 598-608.
23. H. M. J. Wang and I. J. B. Lin, *Organometallics*, 1998, **17**, 972-975.
24. I. J. B. Lin and C. S. Vasam, *Comments Inorg. Chem.*, 2004, **25**, 75-129.
25. P. V. Simpson, B. W. Skelton, P. Raiteri and M. Massi, *New J. Chem.*, 2016, **40**, 5797-5807.
26. C.-h. Chen, Y.-h. Liu, S.-m. Peng, J.-t. Chen and S.-t. Liu, *Dalton Trans.*, 2012, **41**, 2747-2754.
27. D. Canella, S. J. Hock, O. Hiltner, E. Herdtweck, W. A. Herrmann and F. E. Kühn, *Dalton Trans.*, 2012, **41**, 2110-2121.
28. O. Hiltner, F. J. Boch, L. Brewitz, P. Härter, M. Drees, E. Herdtweck, W. A. Herrmann and F. E. Kühn, *Eur. J. Inorg. Chem.*, 2010, 5284-5293.
29. C.-Y. Liu, D.-Y. Chen, G.-H. Lee, S.-M. Peng and S.-T. Liu, *Organometallics*, 1996, **15**, 1055-1061.
30. W. A. Banks, *BMC Neurol.*, 2009, **9**, S3.
31. N. S. M. Vieira, J. C. Bastos, L. P. N. Rebelo, A. Matias, J. M. M. Araújo and A. B. Pereira, *Chemosphere*, 2019, **216**, 576-586.
32. C. Hansch, J. P. Björkroth and A. Leo, *J. Pharm. Sci.*, 1987, **76**, 663-687.
33. W. E. Klunk, Y. Wang, G.-f. Huang, M. L. Debnath, D. P. Holt and C. A. Mathis, *Life Sci.*, 2001, **69**, 1471-1484.
34. W. E. Klunk, B. J. Bacskai, C. A. Mathis, S. T. Kajdasz, M. E. McLellan, M. P. Frosch, M. L. Debnath, D. P. Holt, Y. Wang and B. T. Hyman, *J. Neuropathol. Exp. Neurol.*, 2002, **61**, 797-805.
35. K. K. Skeby, J. Sørensen and B. Schiøtt, *J. Am. Chem. Soc.*, 2013, **135**, 15114-15128.
36. Q. Li, J. Min, Y.-H. Ahn, J. Namm, E. M. Kim, R. Lui, H. Y. Kim, Y. Ji, H. Wu, T. Wisniewski and Y.-T. Chang, *ChemBioChem*, 2007, **8**, 1679-1687.
37. S. A. Hudson, H. Ecroyd, T. W. Kee and J. A. Carver, *FEBS J.*, 2009, **276**, 5960-5972.
38. C. Xue, T. Y. Lin, D. Chang and Z. Guo, *R. Soc. Open Sci.*, 2017, **4**, 160696-160696.
39. L. Racane, R. Stojkovic, V. Tralic-Kulenovic and G. Karminski-Zamola, *Molecules*, 2006, **11**, 325.
40. F. Gao, X. Zhong, Q. Wang, H. Li and S. Zhang, *Chin. J. Chem.*, 2010, **28**, 1057-1068.
41. B. Liu, X. Liu, C. Chen, C. Chen and W. Chen, *Organometallics*, 2011, **31**, 282-288.
42. G. Sheldrick, *Acta Crystallogr. Sect. A: Found. Crystallogr.*, 2008, **64**, 112-122.
43. O. V. Dolomanov, L. J. Bourhis, R. J. Gildea, J. A. K. Howard and H. Puschmann, *J. Appl. Crystallogr.*, 2009, **42**, 339-341.

TOC Figure



View Article Online
DOI: 10.1039/C9DT04687A

